Ultrafast laser inscription of integrated optics 2-telescope beam combiners for K-band interferometry at the CHARA array

Jacopo Siliprandi, David MacLachlan, Calum Ross, Tarun Sharma, Lucas Labadie, et al.

Published version information:

Citation: J Siliprandi et al. Ultrafast laser inscription of integrated optics 2-telescope beam combiners for K-band interferometry at the CHARA array. Proc SPIE 12183 (2022): 1218314. Is in proceedings of: Optical and Infrared Interferometry and Imaging VIII, Montréal, Québec, Canada, 17-23 Jul 2022

DOI: 10.1117/12.2629899

Ultrafast laser inscription of integrated optics 2-telescope beam combiners for K-band interferometry at the CHARA array

Jacopo Siliprandi, David MacLachlan, Calum Ross, Tarun Sharma, Lucas Labadie, et al.

Jacopo Siliprandi, David G. MacLachlan, Calum A. Ross, Tarun K. Sharma, Lucas Labadie, Kalaga Madhav, Abani S. Nayak, Aline N. Dinkelaker, Martin M. Roth, Ettore Pedretti, Theo A. ten Brummelaar, Nicholas J. Scott, Vincent Coudé du Foresto, Robert R. Thomson, Aurélien Benoît, "Ultrafast laser inscription of integrated optics 2-telescope beam combiners for K-band interferometry at the CHARA array," Proc. SPIE 12183, Optical and Infrared Interferometry and Imaging VIII, 1218314 (26 August 2022); doi: 10.1117/12.2629899

Event: SPIE Astronomical Telescopes + Instrumentation, 2022, Montréal, Québec, Canada

Ultrafast laser inscription of integrated optics 2-telescope beam combiners for K-band interferometry at the CHARA array

Jacopo Siliprandi[a,*], David G. MacLachlan[a], Calum A. Ross[a], Tarun K. Sharma[b], Lucas Labadie[b], Kalaga Madhav[c], Abani S. Nayak[c], Aline N. Dinkelaker[c], Martin M. Roth[c], Ettore Pedretti[d], Theo A. ten Brummelaar[e], Nicholas J. Scott[e], Vincent Coudé du Foresto[f], Robert R. Thomson[a], Aurélien Benoit[a,†]

[a]SUPA, Institute of Photonics and Quantum Sciences, Heriot-Watt University, Edinburgh, EH14 4AS
[b]I.Physikalisches Institut der Universität zu Köln, Zülpicher Strasse 77, 50937 Cologne, Germany
[c]Leibniz-Institut für Astrophysik Potsdam, An der Sternwarte 16, 14482 Potsdam, Germany
[d]UKRI STFC Rutherford Appleton Laboratory, Chilton, UK
[e]Center for High Angular Resolution Astronomy, Georgia State University, P.O. Box 3969, Atlanta, Georgia 30302-3969, USA
[f]LESIA of Paris Observatory/CNRS/UPMC/Univ. Paris Diderot, Paris, France

[*]js281@hw.ac.uk; [†]a.benoit@hw.ac.uk.

ABSTRACT

We report the ultrafast laser inscription (ULI) of a 2-telescope integrated optics (IO) beam combiner for K-band interferometry in commercial Infrasil glass. The ULI setup used for this work is based on a 1030 nm femtosecond laser which is paired with a spatial-light-modulator (SLM). The SLM controls the numerical aperture of the focused beam used to write waveguides in the substrate. The optimum ULI parameters were found to inscribe straight single-mode waveguides exhibiting an insertion loss of 1.1 ± 0.1 dB for a 17 mm long chip over the entire K-band. To develop optimal directional couplers, we focused our efforts on investigating the effect of varying the core-to-core separation and the effect of detuning the waveguide parameters in the coupler. By doing so, we have identified fabrication parameters that are suitable for the fabrication of a beam combiner integrating an achromatic 3 dB directional coupler and two photometric taps with a splitting ratio of 80:20. These results demonstrate the capability of the ULI fabrication technique to inscribe efficient achromatic directional couplers in the K-band range. A final fabrication step will involve simple assembly of the beam combiner with input/output fibers in preparation for on-sky testing at the CHARA array planned for July 2022.

Keywords: Astrophotonics, beam combiner, integrated optics, ultrafast laser inscription, CHARA, K-band

1. INTRODUCTION

Since the first demonstration of laser emission in 1960 by Maiman [1], photonic and laser technologies have transformed our society. The field of astronomical instrumentation is now also benefiting from photonic approaches and technologies, and the burgeoning field of "astrophotonics" is beginning to bear fruit. Key examples of astrophotonic technologies currently under development include integrated echelle gratings [2] and the optical fibers used in fiber-fed spectrographs [3-4]. Integrated optics (IO) beam combiners have also enabled impressive demonstrations and are currently exploited at the Very Large Telescope Interferometer (VLTI) with GRAVITY [5] and PIONEER [6]. Nevertheless, current IO beam combiner manufacturing routes are based on silica-on-silicon technology that is optimized for H-band (1.5-1.8 μm) operation, and results in waveguides that exhibit additional losses in K-band (2.0-2.4 μm) due to OH contamination. In addition, this conventional technique cannot be used to access the mid-infrared wavelength range, which is where the important so-called chemical "fingerprint" region lies.

Optical and Infrared Interferometry and Imaging VIII, edited by Antoine Mérand, Stephanie Sallum, Joel Sanchez-Bermudez,
Proc. of SPIE Vol. 12183, 1218314 · © 2022 SPIE · 0277-786X · doi: 10.1117/12.2629899

One manufacturing technology that has the potential to enable the fabrication of integrated optics in a diverse range of optical materials is ultrafast laser inscription (ULI), and ULI has already been used to manufacture devices for a range of astrophotonic applications [7-11]. Recently, ULI has been used to inscribe K-band waveguide components in commercial Infrasil glass (IG) which exhibits improved transparency in the K-band compared to standard fused silica. In this work, an efficient asymmetric directional coupler was reported to exhibit a 3 dB splitting ratio (50:50) with a high interferometric contrast of 92 % [12], a figure similar to that of the K-band interferometric instrument, GRAVITY at VLTI, that has demonstrated an impressive contrast of 95 % [13].

In this paper, we report on the development and fabrication of a 2-telescope beam combiner in a 17 mm square IG chip. The beam combiner is composed of three asymmetric directional couplers; a 3 dB (50:50) coupler for interferometry, and two photometric taps with a splitting ratio of around 80:20. In the near future, this device will be permanently connected to input/output fibre V-grooves to enable a packaged 2-telescope K-band IO beam combiner which we intend to test at the CHARA array in July 2022 [14-15].

2. ULI OF EFFICIENT K-BAND SINGLE MODE WAVEGUIDES

The ULI fabrication system is based on a Light Conversion PHAROS laser that delivers 185 fs pulses of 1030 nm light with a repetition rate of 500 kHz. The setup also integrates a spatial-light-modulator (SLM) (Hamamatsu, LCOS-SLM X13138) and writing objective with a maximum numerical aperture of 0.67 (OptoSigma, PAL-50-NIR-HR-LC00). The SLM allows us to arbitrarily control the size of the laser beam entering the objective lens, and hence control of the effective NA of the focus used to fabricate waveguides. All waveguides were fabricated using the multiscan technique [16,17] with a scan separation of 200 nm and a substrate translation speed of 4 mms^{-1}. Our ULI investigation spanned a range of number of scans, from 25 to 37 in steps of 2, pulse energies, from 60 to 177 nJ in incremental steps of +7 %, and effective NAs from 0.45 to 0.6 in steps of 0.05.

The waveguide characterization setup utilizes a supercontinuum source (SC) (NKT Extreme-K), the bandwidth of which is filtered by a K-band bandpass filter centred on 2250 ± 250 nm (Thorlabs FB2250-500). This filtered light is then coupled into a 1 m commercial single-mode fiber (Nufern SM1950) that is used to butt-couple light into the waveguide under test. Initially, the effect of varying the effective NA used to fabricate waveguides was investigated by measuring the insertion losses with a simple thermal power meter (Thorlabs SC305), Fig. 1(a). After optimum ULI parameters were found, the insertion loss of the optimal waveguide across the K-band was investigated by replacing the thermal power meter with a broadband optical spectrum analyzer (OSA) (Thorlabs OSA205) [12], as shown in Fig. 1(b). Figure 1 presents the main results of the straight waveguide investigation showing the loss evolution as a function of the pulse energy for all the effective NAs (Fig 1(a)), as well as the insertion losses of the best waveguide (Fig 1(b)).

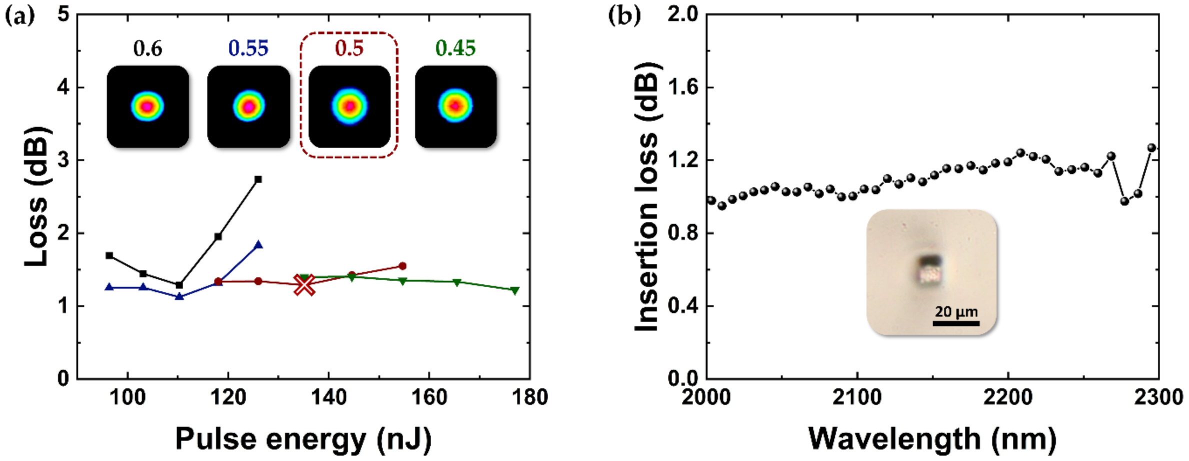

Figure 1. (a) Evolution of the waveguide insertion loss as a function of the focused pulse energy written with 31 scans for the effective NAs: 0.6 (black squares), 0.55 (blue upward triangles), 0.5 (red dots), 0.45 (green downward triangles). Inset: Near-field intensity pattern of best waveguide for each NA. The red cross and dashed rectangle highlight the measurement obtained at 135 nJ for the selected NA of 0.5. (b) Evolution of the insertion losses of the best straight waveguide as a function of the wavelength where each point represents a raw data average of ± 4 nm. Inset: scaled micrograph of the ULI waveguide.

The optimum ULI parameters were judged to be those that minimized the insertion loss, but also enabled stable and repeatable fabrication. For this reason, the optimum parameters were determined to be a pulse energy of 135 nJ when using a NA of 0.5 and 31 scans, as represented by the red cross in Fig. 1(a). Figure 1(b) shows the insertion loss as a function of the wavelength for this waveguide, showing an average value of 1.1 ± 0.1 dB between 2 and 2.3 µm, corresponding to a global throughput of ~78 %. All spectra were measured using the highest OSA resolution and sensitivity setting, which provided 6806 raw data points over the whole K-band with a spectral resolution of 0.25 cm^{-1}, a spectral accuracy of ± 2 ppm, and a level sensitivity of – 40 dBm/nm for an optical path difference (OPD) of ± 4 cm. Each black point in Fig. 1(b) is an average over a wavelength span of ± 4 nm. Furthermore, as one can observe in Fig. 1, the whole K-band (2.0-2.4 µm) cannot be fully characterized due to insufficient light intensity from the SC source after 2.3 µm. A bend loss study was also performed, demonstrating negligible additional losses when a waveguide undergoes a transverse deviation of 59.5 µm over a length of 3.5 mm, corresponding to a minimum radius of curvature of ~42 mm.

3. ULI FABRICATION OF A 2-TELESCOPE IO BEAM COMBINER

3.1 Development of achromatic directional couplers

A study was performed to develop couplers capable of achromatic splitting ratios of 50:50 and 80:20. To achieve this, we investigated the effect of varying two key parameters: the waveguide core-to-core (CC) separation and the sizes of the waveguides in the interaction region. The former can be used to control the strength of the coupling between the two waveguides in the interaction region, while the latter regulates the detuning of the coupled modes, and thus allows us to achieve evanescent couplers that are more achromatic [18-19].

Figure 2(a) shows a schematic of an asymmetric directional coupler fabricated for our study, where the input optical power $P_0(\lambda)$ is coupled in Arm 1 and the two output powers $P_{A1}(\lambda)$ and $P_{A2}(\lambda)$ are recorded with the OSA. The mode coupling between the two arms occurs in the interaction region where the two arms are sufficiently close for the evanescent tails of the modes to partially overlap with each other. To characterize the directional coupler behavior, we determined the splitting ratio of the directional coupler by calculating the fraction of input power that is in the same input waveguide after splitting with the power ratio formula: $R_1(\lambda) = P_{A1}(\lambda) / (P_{A1}(\lambda) + P_{A2}(\lambda))$. Our goal is to tune the asymmetric directional couplers while maintaining the necessary splitting ratios. To achieve this, the couplers were designed using two principles: (i) each arm of the coupler is created from two counterposing S-shaped bends with no straight interaction length, (ii) the width of the waveguides in the interaction region are mismatched to achieve the desired detuning in the propagation constants. The waveguide width is increased in Arm 1 while the waveguide in Arm 2 is detuned to a smaller size, when compared to the other arm, to correctly detune the propagation constants of the waveguides and, thus, produce a more achromatic coupling ratio across the K-band. The evolution of waveguide widths in the interaction region is described in Fig. 2(a) with Arm 1 exhibiting a width W', wider than the optimum width w, while the detuned waveguide in Arm 2 shows a smaller width W'_D, where $W'_D = D \cdot W'$ with $D < 1$ the detune parameter. The width W' was determined experimentally by studying the beam quality of wider than optimum waveguides fabricated by increasing the scan separation to produce waveguide widths in increments of 10 %. In this way, the maximum waveguide width $W' = 1.2 \cdot w$ which maintained single-mode beam quality was selected.

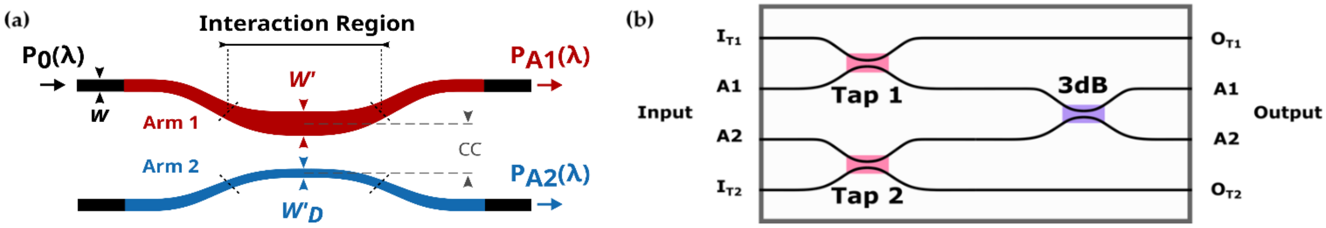

Figure 2. (a) Schematic of an asymmetric directional coupler with a description of the width evolution of the waveguide from w (black) to the larger W' (red) and the detuned waveguide W'_D (blue) with the detune parameter D in the interaction region. (b) Representation of the final beam combiner composed of three asymmetric directional couplers with two photometric taps (pink) and a 3 dB coupler (purple) with the labels Input/Output.

Based on the optimum ULI parameters presented in the previous sections and the directional coupler design, a first investigation was performed on the CC separation, the key parameter that controls the energy transfer between the two waveguides, from 8 µm to 13 µm in steps of 1 µm. Figure 3(a) presents the 2D map that summarizes the experimental results of the CC study by representing the evolution of the splitting ratio $R_1(\lambda)$ (fraction of power which propagates in the input waveguide) as a function of the CC separation, where both waveguides present the same width *W'* in the interaction region (D = 1 for Arm 2). One can observe a flatter splitting ratio over the whole wavelength span for the smaller CC separations. Then, we inscribed directional couplers with CC separations ranging from 8 μm to 11 μm while also detuning Arm 2 width W'_D to perform a detuned coupler investigation and acquire the desired asymmetric behavior. Figure 3(b) presents the 2D map of $R_1(\lambda)$ as a function of the wavelength and the detune parameter *D* for a CC separation of 9 μm. One can observe a clear achromatic splitting ratio for the smaller detune parameters over the whole wavelength span. In particular, with a CC of 9 μm, the two desired splitting ratios were found with D = 0.6 and D = 0.7 for the 3 dB asymmetric directional couplers and the photometric tap respectively. Also, one can highlight an interesting point from Fig. 3(b) on the global behavior of the beam combiner. Indeed, the photometric tap couplers, written with a detune parameter D = 0.7, shows that 80 % of the incoming light is transferred in the opposite arm of the described asymmetric directional coupler. It is crucial to highlight that this splitting ratio behavior implies that to obtain a maximum of optical power in the 3 dB couplers for interferometry measurements (A1 and A2 waveguides), the two inputs from the telescopes must be coupled in the two outer waveguides, labeled I_{T1} and I_{T2} in the beam combiner schematically represented in Fig. 2(b). These experimental results demonstrate the capability of the ULI fabrication technique to inscribe efficient asymmetric directional coupler with the desired splitting ratio in the K-band spectrum range.

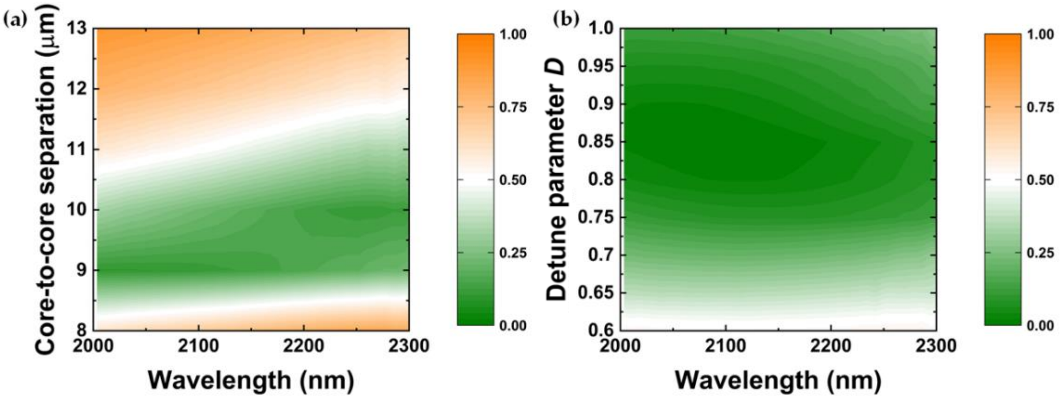

Figure 3. (a) 2D heat map representing the experimental measurements providing the $R_1(\lambda)$ as a function of the core-to-core separation and the wavelength. (b) 2D heat map representing the experimental measurements that provide the $R_1(\lambda)$ of the detuned coupler investigation for directional couplers with a core-to-core separation of 9 μm.

3.2 Beam combiner fabrication

A complete beam combiner was fabricated based on the results from the ULI parameter and coupler optimization studies. The same setup described above was used to characterize the beam combiner, except now we measured three optical powers per input to fully characterize the splitting ratios. To do so, light from the SC was coupled into I_{T1} (I_{T2}) and the optical powers were measured at outputs of O_{T1}, A1, and A2 (O_{T2}, A1, and A2). Figure 4 presents the results of the beam combiner characterization experiments, by describing the power ratio evolution $R_1(\lambda)$ and $R_2(\lambda)$ of the 3 dB coupler (a, b) and the photometric tap coupler Tap 1 (c) and Tap 2 (d).

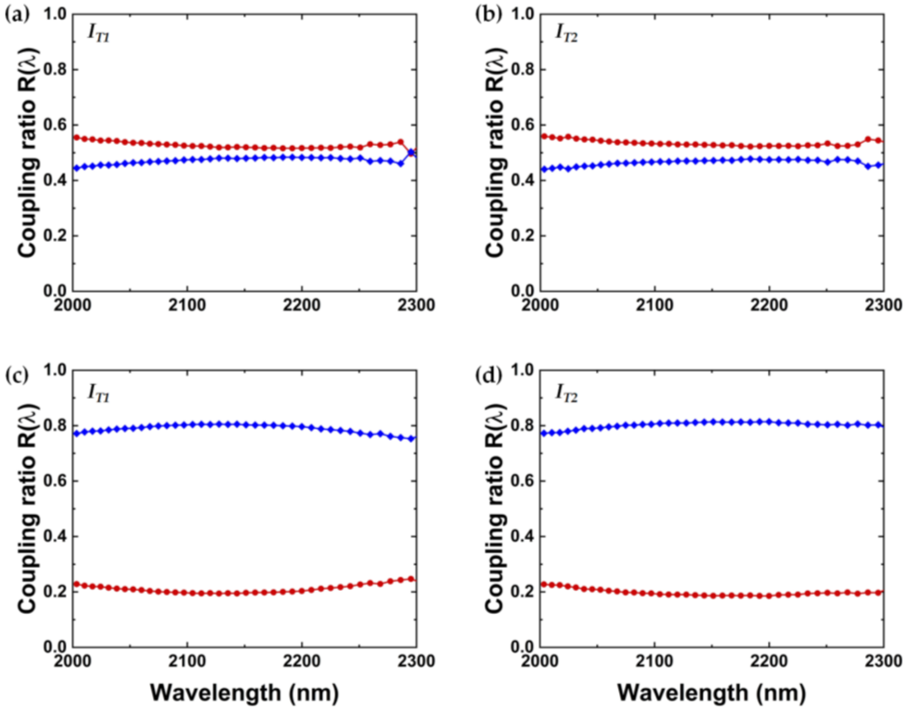

Figure 4. (a-d) Coupling ratio R1(λ) (red dots) and R2(λ) (blue diamonds) of an ultrafast laser inscribed beam combiner characterized by coupling input light in the inputs I_{T1} and I_{T2} to obtain two experimental measurements of the 3 dB asymmetric directional coupler (a, b) and one for each photometric asymmetric tap directional coupler, labeled Tap 1 (c) and Tap 2 (d).

4. CONCLUSIONS

We report on the development and the fabrication of a 2-telescope prototype K-band beam combiner by ultrafast laser inscription. We used an SLM to correctly tune the effective NA of the focused laser used to inscribe waveguides. The optimum waveguide fabrication was found to exhibit a low insertion loss of 1.1 ± 0.1 dB, corresponding to a global throughput of ~78 % over the K-band in a 17 mm long substrate of commercial Infrasil glass. Subsequently, we developed achromatic evanescent field couplers by minimizing the bend losses, studying the effect of core-to-core separation, and by investigating the effect of detuning the waveguide properties in the coupler interaction region. The resulting set of ULI parameters was established to provide the two desired splitting ratios for the asymmetric directional couplers required by the full-beam combiner. Finally, a 2-telescope IO beam combiner was fabricated with three achromatic directional couplers: a 3 dB coupler for interferometric measurements and two photometric taps with a splitting ratio around 80:20 for calibration, which are in good agreement with the initial specifications. The final step will involve connecting input/output fiber V-grooves to update K-band interferometric instruments at the CHARA array.

5. ACKNOWLEDGEMENTS

RRT thanks UKRI-EPSRC and UKRI-STFC for support through research grants: EP/T020903/1, ST/V000403/1, EP/P027415/1, EP/S000410/1, ST/N000625/1. JS's PhD studentship was part-funded by the EU Quantum Flagship through the "PhoG – Sub-Poissonian Photon Gun by Coherent Diffusive Photonics" project. RRT thanks Light Conversion for their support. KM, MMR, ASN, and AD were supported from BMBF grant 03Z22AN11 "Astrophotonics", and BMBF grant 03Z22AI1 "Strategic Investment", at the Zentrum für Innovationskompetenz innoFSPEC.

REFERENCES

[1] Maiman, T. H., “Optical and microwave-optical experiments in Ruby,” PRL **4**(11) (1960).

[2] Stoll, A., Wang, Y., Madhav, K., “Integrated echelle gratings for astrophotonics," Proc. SPIE 11203, 112030Z (2020).

[3] Mayor, M., Pepe, F., Queloz, D., et al., “Settings new standards with HARPS,” The Messenger, 114, 20-24 (2003).

[4] Bluhm, P., Luque, R., Espinoza, N., et al., “Precise mass and radius of a transiting super-Earth planet orbiting the M dwarf TOI-1235: a planet in the radius gap?” A&A **639**, A132 (2020).

[5] Eisenhauer, F., Perrin, G., Brandner, W., et al., “GRAVITY: Observing the universe in Motion,” The Messenger, **143**, 16-24 (2011).

[6] Benisty, M., Berger, J.-P., Jocou, L., et al., “An integrated optics beam combiner for the second generation VLTI instruments,” A&A **498**(2) 601-613 (2009).

[7] MacLachlan, D. G., Harris, R. J., Gris-Sanchez, I., et al., “Efficient photonic reformatting of celestial light for diffraction-limited spectroscopy,” MNRAS **464**(4), 4950–4957 (2016).

[8] Butcher, H. L., MacLachlan D. G., Lee David, et al., “Ultrafast laser-inscribed mid-infrared evanescent field directional couplers in GeAsSe chalcogenide glass,” OSA Continuum **1**(1), 221-228 (2018).

[9] Arriola, A., Mukherjee, S., Choudhury, D., et al., “Ultrafast laser inscription of mid-IR directional couplers for stellar interferometry,” Opt. Lett. **39**(16), 4820-4822 (2014).

[10] Nayak, A. S., Labadie, L, Sharma, T. K., et al., “First stellar photons for an integrated optics discrete beam combiner at the William Herschel Telescope", Nayak, App. Opt. **60**(19), D129-D142 (2021).

[11] Nayak, A. S., Poletti, T., Sharma, T. K., et al., "Chromatic response of a four-telescope integrated-optics discrete beam combiner at the astronomical L band," Opt. Exp. **28**(23), 34346-34361 (2020).

[12] Benoit, A., Pike, F. A., Sharma, T. K., et al., “Ultrafast laser inscription of asymmetric integrated waveguide 3 dB couplers for astronomical K-band interferometry at the CHARA array,” JOSA B **38**(9) 2455-2464 (2021).

[13] Perraut, K., Jocou, L., Berger. J. P., et al., “Single-mode waveguides for GRAVITY - I. The cryogenic 4-telescope integrated optics beam combiner” A&A **614**, A70 (2018).

[14] Lhomé, E., Scott, N., ten Brummelaar, T., et al., “JouFLU: an upgraded FLUOR beam combiner at the CHARA Array,” Proc. SPIE 8445, 88452I (2012).

[15] ten Brummelaar, T. A., McAlister, H. A., Ridgway, S. T., et al., “First Results from the CHARA Array. II. A Description of the Instrument,” ApJ **628**, 453-465 (2005).

[16] Nasu, Y., Kohtoku, M., and Hibino, Y., “Low-loss waveguides written with a femtosecond laser for flexible interconnection in a planar light-wave circuit” Opt. Lett. **30**(7), 723-725 (2005).

[17] Brown, G., Thomson, R. R., Kar, A. K., et al., “Ultrafast laser inscription of Bragg-grating waveguides using the multiscan technique,” Opt. Lett. **37**(4), 491-493 (2012).

[18] Takagi, A., Jinguji, K., and Kawachi, M., “Design and Fabrication of Broad-Band Silica-Based Optical Waveguide Couplers with Asymmetric Structure” IEEE Journ. Qunt. Elec. **28**, 848-855 (1992).

[19] Chen, W.-J., Eaton, S. M., Zhang H., et al., “Broadband directional couplers fabricated in bulk glass with high repetition rate femtosecond laser pulses” Opt. Exp. **16**(15), 11470-11480 (2008).